AIP | Journal of Applied Physics

A method to enhance the data transfer rate of eutectic Sb-Te phase-change recording media

Tung-Ti Yeh, T.-E. Hsieh, and Han-Ping D. Shieh

Citation: Journal of Applied Physics **98**, 023102 (2005); doi: 10.1063/1.1957132
View online: http://dx.doi.org/10.1063/1.1957132
View Table of Contents: http://scitation.aip.org/content/aip/journal/jap/98/2?ver=pdfcov
Published by the AIP Publishing

JOURNAL OF APPLIED PHYSICS **98**, 023102 (2005)

A method to enhance the data transfer rate of eutectic Sb-Te phase-change recording media

Tung-Ti Yeh and T.-E. Hsieh[a]
Department of Materials Science and Engineering, National Chiao-Tung University,
1001 Ta-Hsueh Road, Hsinchu 30050, Taiwan, Republic of China

Han-Ping D. Shieh
Department of Photonics and Institute of Electro-Optical Engineering, National Chiao-Tung University,
1001 Ta-Hsueh Road, Hsinchu 30010, Taiwan, Republic of China

(Received 23 August 2004; accepted 24 May 2005; published online 19 July 2005)

This work describes the effect of nitrogen doping to eutectic Sb-Te phase-change materials in order to enhance the speed of the amorphous-to-crystalline phase transformation. When nitrogen at a sputtering gas flow ratio of $N_2/Ar=3\%$ was doped in the eutectic Ge-In-Sb-Te recording layer, the data transfer rate was increased up to 1.6 times. When thin GeN_x nucleation promotion layers were further added in below and above the recording layer, an overall enhancement up to 3.3 times in data transfer rate was achieved. The nitrogen contents corresponding to the N_2/Ar flow ratios ($N_2/Ar =0\%–10\%$) were calibrated by electron spectroscopy for chemical analysis. Transmission electron microscopy revealed that nitrogen doping was able to promote the phase transformation by generating numerous nucleation sites uniformly distributed in the recording layer and hence increased the recrystallization speed. *© 2005 American Institute of Physics.*
[DOI: 10.1063/1.1957132]

I. INTRODUCTION

A large storage capacity and a high data transfer rate are always demanded for optical recording media. The phase-change recording materials with higher amorphous-crystalline transition speed are hence required. Currently the eutectic Sb-Te system, or called the fast-growth phase-change alloy, has received much attention because of its good signal properties and high recrystallization speed when short-wavelength laser and high numerical aperture (NA) lenses are used. The eutectic Sb-Te system is termed as the fast-growth material since its recrystallization is initiated from the crystalline-amorphous interface and the amorphous mark shrinks as the grain growth propagates toward the center of the signal marks,[1–4] as illustrated in Fig. 1(a). Adding foreign element in the eutectic Sb-Te system such as Ag, In, and Ge is a common way to improve the recrystallization characteristics and optical properties of optical disks.[5] Not only the composition of the recording material but also the nucleation-promoting layer/dielectric layers enclosing the recording layer play important roles in the recrystallization process.[6,7] The surface reactivity and chemical affinity are the major factors that enhance the recrystallization speed. In this work, we doped nitrogen during the sputter deposition of the recording material and inserted GeN nucleation-promotion layers above and below the recording layer in order to further enhance the data transfer rate of eutectic Sb-Te phase-change optical disk. The signal properties and data transfer rate of optical disks were investigated by using a dynamic test. The nitrogen contents doped in the recording layer at various sputtering N_2/Ar flow ratios were determined by electron spectroscopy for chemical analysis (ESCA) and transmission electron microscopy (TEM) was utilized to examine the change in the microstructure induced by nitrogen doping.

II. THE MODEL OF RECRYSTALLIZATION PROCESS

Figure 1(b) illustrates the model applied to enhance the velocity of phase transformation. It was realized by doping nitrogen in the eutectic Ge-In-Sb-Te recording layer as well as in the nucleation promotion layers. Nitrogen doping generates numerous nanometer-scale precipitates uniformly distributed in the recording layer. They provide the preferential sites for amorphous-crystalline transition in the recording layer so that the edge of marks is not the only site to initiate the recrystallization during signal recording. The tiny pre-

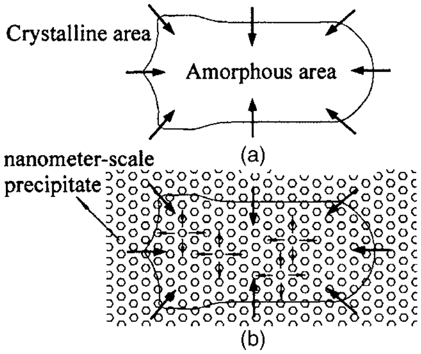

FIG. 1. (a) In phase-change recording materials with a growth-dominated crystallization mechanism, crystallization starts from the crystalline-amorphous mark edges and proceeds to the center of the mark. (b) In nitrogen-doped fast-growth materials, it is assumed that the phase transition initiates both at the crystalline-amorphous mark edges and precipitates within the mark.

---

[a] Author to whom correspondence should be addressed; electronic mail: tehsieh@cc.nctu.edu.tw

0021-8979/2005/98(2)/023102/5/$22.50

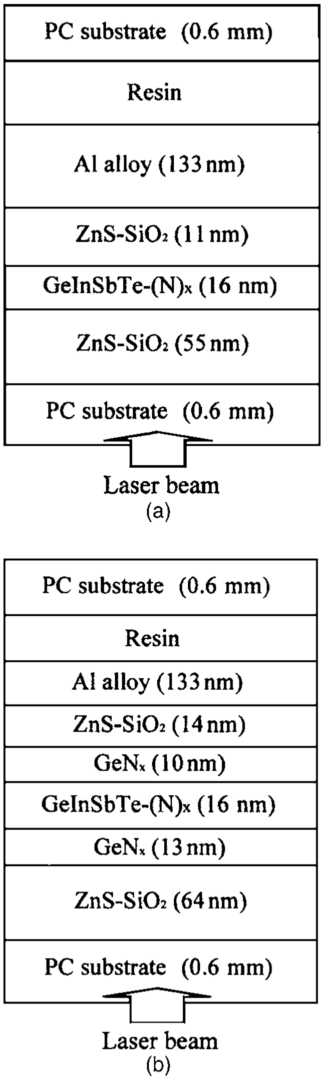

FIG. 2. The cross-sectional structures of an optical disk with (a) four-layer and (b) six-layer stack.

cipitates not only induce the heterogeneous nucleation, they also shorten the distance of grain growth required to complete the transition. Hence the velocity of amorphous-crystalline transition is promoted. In addition, the precipitates must remain stable under laser irradiation to ensure good disk signal properties after periodic signal recording.

III. EXPERIMENTAL PROCEDURES

Figure 2 illustrates the multilayer structures of the optical disk used in this work. At first, disk samples with conventional four-layer stack were prepared using a SFI (Surface Interface Corp.) sputtering system at a background pressure better than 1×10^{-6} torr. The multilayer structure was deposited on 0.6-mm-thick polycarbonate (PC) substrate in the sequence of ZnS-SiO$_2$(55 nm)/Ge-In-Sb-Te (GIST)-(N)$_x$(16 nm)/ZnS-SiO$_2$(11 nm)/Al-Cr(133 nm), as shown in Fig. 2(a). During the deposition of the recording layer, the N$_2$/Ar flow ratio was adjusted to values of 0%, 0.5%, 1%, 3%, 5%, and 10% to obtain undoped and nitrogen-doped specimens. Then the optimal composition of GIST-(N)$_x$ was chosen to be the recording layer of the optical disk with six-layer stack shown in Fig. 2(b). The sputtering conditions and designated sample numbers are listed in Table I.

TABLE I. Sputtering conditions and designated sample numbers.

Sample no.	N$_2$/Ar ratio	Target type	Sputtering pressure (mTorr)	Sputtering power (W)
	0/10	ZnS-SiO$_2$	3	250 (rf)
	0/10	Al-Cr	3	400 (dc)
	20/10	Ge	3	200 (rf)
N000	0/10	GeInSbTe	3	50 (rf)
N005	0.05/10 (0.5%)	GeInSbTe	3	50 (rf)
N010	0.1/10 (1.0%)	GeInSbTe	3	50 (rf)
N030	0.3/10 (3.0%)	GeInSbTe	3	50 (rf)
N050	0.5/10 (5.0%)	GeInSbTe	3	50 (rf)
N100	1.0/10 (10.0%)	GeInSbTe	3	50 (rf)

After the optimum initialization, the disk samples were sent to a dynamic tester (DDU1000, PULSTEC Co.) having a pickup head with a 650-nm laser diode and a NA=0.6 objective lens to evaluate their signal properties. Figure 3 shows the writing strategy used in this study. At the beginning of the dynamic test, the disks were written at various laser powers (7–15 mW) with fixed erasing power (P_e =6 mW) and reading power (P_r=0.7 mW) at various linear velocities to identify the optimum writing power (P_w). Then the tracks recorded with 8T signals were erased by irradiating a dc laser beam of various laser powers (3–7 mW) at the same linear velocity used for recording. The carrier-to-noise ratio (CNR) was measured before and after the erasing process to determine the attenuation of 8T signal carrier, and the value of the attenuation of 8T signal carrier is defined as the dc erasability.

The nitrogen contents of GIST-(N)$_x$ recording layer corresponding to various N$_2$/Ar flow ratios were calibrated by ESCA (Thermo VG-Scientific, Microlab 350). The method report by Nokukuni *et al.*[8] and Chen *et al.*[9] was adopted to prepare the plan-view TEM (PTEM) specimens. After removing the PC substrate, the disk sample was cut into small pieces using a pair of scissors. A 3M tape was applied to the disk to peel off the Al-Cr reflection layer. After dissolution of the PC substrate by CH$_2$Cl$_2$ solution, the specimen was mounted on the copper mesh and transferred to a TEM (Philips, Tecnai 20 TEM) for microstructure observation.

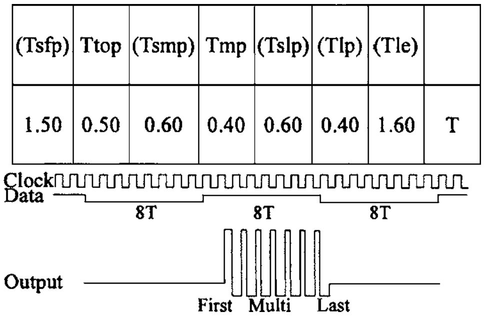

FIG. 3. Writing strategy for 8T signal. (Tsfp: start-up delay value for the first pulse. Ttop: ending delay value for the first pulse, Tsmp and Tmp: delay time, Tslp: start-up delay value for the last pulse, Tlp: ending delay value for the last pulse, and Tle: start-up delay for the off pulse)

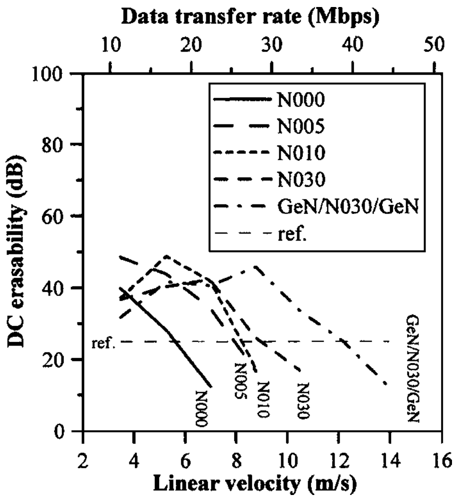

FIG. 4. dc erasability of 8T signals as a function of linear velocity and/or data transfer rate of various samples (the 8T carriers were written on the initialized track at optimum writing power before erasing).

IV. RESULTS AND DISCUSSION

A. dc erasability

Figure 4 shows the dc erasability of 8T signals as a function of linear velocity and/or data transfer rate of various samples. The outputs of dc laser power were adjusted so that the dc erasability at each linear velocity reached the maximum. As we know, the dc erasability higher than 25 dB is required for the direct overwriting (DOW) of optical disks.[10] Furthermore, dc erasability of each disk sample significantly decreased with an increase in linear velocity. This result was attributed to the fact that the laser irradiation time at a high linear velocity is shorter than that at a low linear velocity. Laser irradiation time at a specific linear velocity is expressed as[11]

$$T = \frac{D}{V}, \tag{1}$$

where T is the laser irradiation time, D is the diameter of the laser spot, and V is the linear velocity of the disk. Equation (1) depicts that a recording material must possess a sufficiently high recrystallization speed for phase change so that amorphous marks can be effectively erased at a specific linear velocity. Therefore, it is necessary for a phase-change optical disk to have a high recrystallization speed to realize a high data transfer rate. From the results of dc erasability test shown in Fig. 4, the doping-free disk sample (N000) just passes the test requirement at a linear velocity below 5.3 m/sec. However, the nitrogen-doped samples, for instance, the N030 and GeN/N030/GeN disk samples successfully pass the dc erasability test requirement at a linear velocity of 8.8 and 12.3 m/sec, respectively. This means that the recrystallization speeds of N030 and GeN/N030/GeN disk samples were approximately 1.6 and 3.3 times higher than that of the sample free of nitrogen. Apparently, an appropriate amount of nitrogen doping and an effective nucleation-promoting layer benefited the data transfer rate and/or recrystallization speed of GIST phase-change optical disks. Miao *et al.*[12] proposed that the GeN layers might cause heterogeneous nucleation at the interface of GeN and phase-change recording layer to enhance the recrystallization speed.

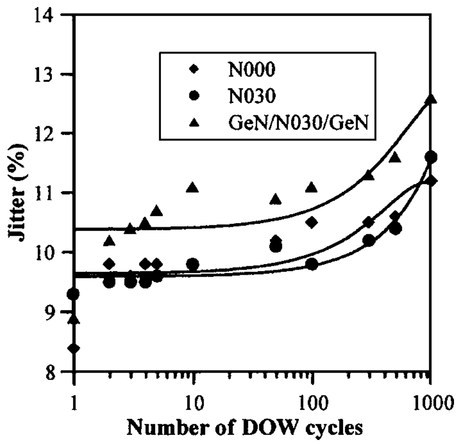

FIG. 5. Jitter values of random data vs the number of DOW cycles at a linear velocity of 3.5 m/sec for N000, N030, and GeN/N030/GeN disk samples.

B. Jitter values

The method of digital versatile disk (DVD) jitter evaluation was adopted to measure the jitter for all intervals between the data and the clock.[13] The random data was written in the track of N000, N030, and GeN/N030/GeN disk samples at 3.5-m/sec linear velocity for measuring the jitter values. A low jitter implies a very low error when 8T signal marks were written in the disk samples. Figure 5 shows the jitter values of N000, N030, and GeN/N030/GeN disk samples for various DOW cycles. It was found that N000 and N030 samples have quite similar jitter values at the same number of DOW cycles. This implies that a relatively small amount of nitrogen doping would not deteriorate the signal properties of optical disks. GeN/N030/GeN sample exhibited higher jitter value than N000 or N030 samples at the same number of DOW cycles. This might result from the difference in the thermal properties between GeN/N030/GeN and N000 (or N030) disks because of the different disk structures.

C. Nitrogen concentration analyzed by ESCA

The nitrogen contents of GIST-$(N)_x$ recording layer corresponding to various N_2/Ar flow ratios (0%–10%) shown in Fig. 6 were calibrated by ESCA. It was found that the nitrogen content increases with the increase of N_2/Ar flow ratio and similar result was reported by Jeong *et al.*[14] when $Ge_2Sb_2Te_5$ recording material was sputtered at the sputtering gas flow ratio of $N_2/Ar \leq 10\%$.

D. TEM observation

The micrographs of 8T signal marks in disk samples of N000 and N030 written at a linear velocity of 7 and 10.5 m/sec are shown in Figs. 7(a) and 7(b). The lamellar-like structure commonly seen in a eutectic recording alloy was observed in the crystalline area of both samples. In addition to the higher degree of structure irregularity, we observed

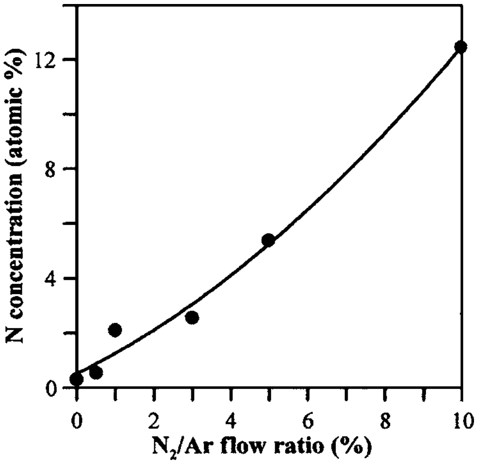

FIG. 6. Nitrogen content of GIST-$(N)_x$ recording layer vs N_2/Ar gas flow ratio of sputter deposition.

tiny precipitates uniformly distributed in N030 sample at high magnification. These precipitates with size less than 10 nm were considered to be nitride compounds, e.g., Ge-N, Sb-N, Te-N, In-N, etc. The 8T amorphous marks were formed at an optimum P_w/P_e and the amorphous marks in N000 sample possess a more distinctive shape than those in N030 sample. Figures 7(c) and 7(d) show the micrographs of the residual marks in N000 and N030 samples, respectively, erased at the linear velocities of 7 and 10.5 m/sec. As shown in Figs. 7(c) and 7(d), the residue of marks can be easily found in the undoped sample while in the nitrogen-doped specimens, the residual marks were hardly observed and entirely different from that of the undoped sample, as shown in Fig. 7(c). This explains why the dc erasability of an undoped sample is inferior to that of nitrogen-doped samples, as shown in Fig. 5. The microstructure observation also revealed that the recrystallization behavior of the nitrogen-doped specimens should be different from that of the undoped specimen due to the existence of tiny nitride precipitates.

E. Calculation of activation energy E_a of phase transition

The eutectic GIST alloy is termed as the fast-growth material since its recrystallization is initiated from the crystalline-amorphous interface and the amorphous mark shrinks as the grain growth propagates toward the center of the mark, as illustrated in Fig. 1(a). The velocity of the grain growth derived from the net jump frequency of atoms across the amorphous-crystallization interface can be expressed as[3]

$$V(T) = V_0 e^{-E_a/R\Delta T}(1 - e^{-\Delta g^{ac}/RT}), \qquad (2)$$

where V_0 is a preexponential factor, E_a is the activation energy of transition from the amorphous to the crystalline state, Δg^{ac} is the free energy difference between an atom in the amorphous state and that in the crystalline state, R is the gas constant, and ΔT is the temperature difference between the interface temperature and the glass transition temperature. Equation (2) implies that low E_a value benefits the phase transition from the amorphous state to the crystalline state.

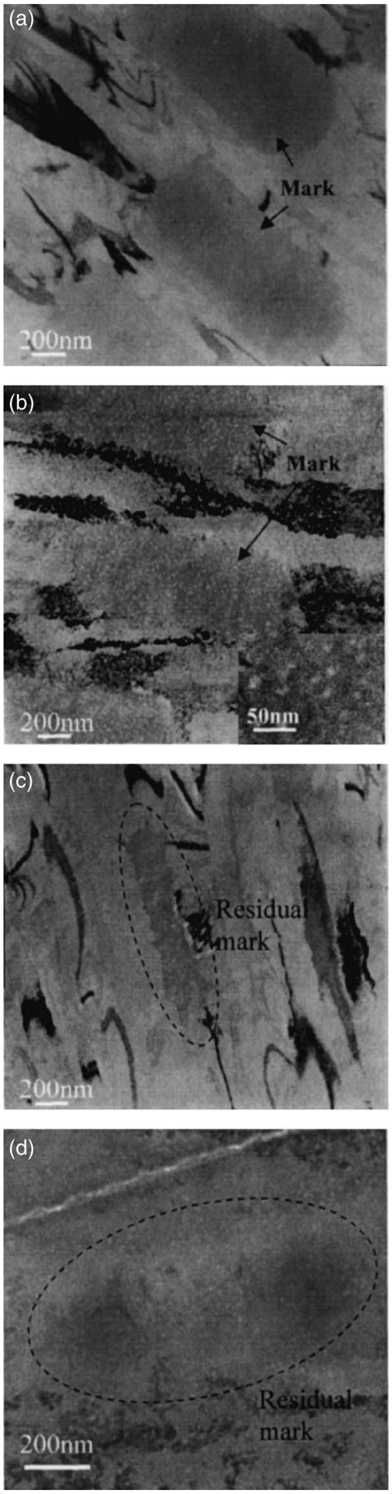

FIG. 7. The micrographs of 8T signal marks of (a) N000 disk sample written at a linear velocity of 7 m/sec and (b) N030 disk sample written at a linear velocity of 10.5 m/sec. The micrographs of residual amorphous marks of (c) N000 disk sample erased at a linear velocity of 7 m/sec and (d) N030 disk sample erased at a linear velocity of 10.5 m/sec. A local magnified picture of (b) is attached at the lower right-hand corner of the micrograph.

We measured five different crystallization temperatures at different heating rates (5, 10, 20, 40 and 80 °C/min) using differential scanning calorimetry (DSC, Dupont 2000 Series) to fit into the Kissinger plot[15,16] shown in Eq. (2) to calculate the activation energy for crystallization. The Kissinger equation is

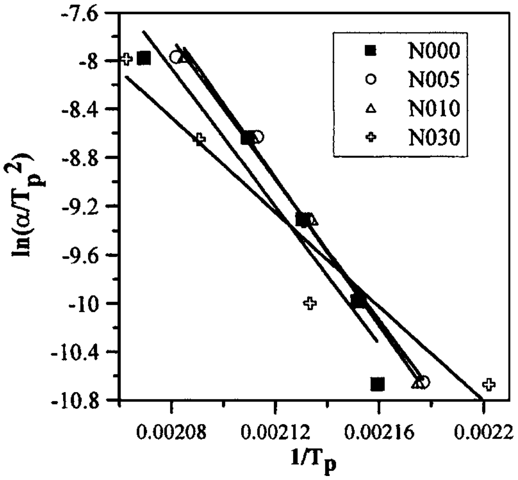

FIG. 8. The Kissinger plot of N000, N005, N010, and N030 samples.

$$\ln\left(\frac{\alpha}{T_P^2}\right) = -\left(\frac{E_a}{R}\right)T_P^{-1} + c, \tag{3}$$

where α is a heating rate, T_P is the crystallization temperature, E_a is the activation energy for phase transformation, R is the Boltzamann constant, and c is a constant. The activation energy of transition from the amorphous to the crystalline state, E_a, can be calculated from the slope of the plot of $\ln(\alpha/T_p^2)$ vs $1/T_p$ shown in Fig. 8. For N000, N005, N010, and N030 samples, E_a were 2.462, 2.521, 2.642, and 1.686 eV, respectively, as shown in Table II. According to the recrystallization model shown in Fig. 1(b), nitrogen doping might generate numerous nanometer-scale precipitates uniformly distributed in the GIST recording layer. In addition to the amorphous-crystalline edge of marks, they were also the preferential sites for the amorphous-crystalline transition of the recording media. When sufficient numbers of tiny precipitates provided the sites for heterogeneous nucleation, a substantial decrease of E_a was hence observed, e.g., in N030 sample. Furthermore, uniform distribution of precipitates also shortened the distance of grain growth required to complete the transition so that an enhancement of recrystallization speeds/data transfer rate was obtained.

TABLE II. Calculation of the activation energy for N000, N005, N010, and N030 samples.

Sample no.	N000	N005	N010	N030
Activation energy (eV)	2.462	2.521	2.642	1.686

V. CONCLUSIONS

We added nitrogen during sputter deposition of Sb-Te phase-change recording material in order to enhance the rate of amorphous-to-crystalline phase transformation. As revealed by TEM observation, nitrogen doping was able to provide numerous nanometer-scale precipitates in the recording layer, which could serve as the preferential sites of heterogeneous nucleation for amorphous-crystalline transition. In addition to the edge of the signal marks, these tiny precipitates were also the sites to initiate the recrystallization of recording media so that the data transfer rate of optical disks was effectively increased. Nitrogen doping at a sputtering gas flow ratio of $N_2/Ar = 3\%$ (corresponds to about 3 at. % of nitrogen doping as determined by ESCA) might enhance the data transfer rate of an optical disk up to 1.6 times without severely damaging the signal jitter values. However, the disks failed the dynamic tests when too much nitrogen ($N_2/Ar \geqslant 5\%$) was introduced. Further enhancement of the data transfer rate up to 3.3 times was achieved in the phase-change optical disk in which the GIST-$(N)_x$ recording layer was enclosed between two GeN_x nucleation promotion layers. The implantation of new nucleation sites not only accelerated the recrystallization speed of amorphous-crystalline transition via heterogeneous nucleation, it also shortened the distance of grain growth so that the phase-change optical disks with high data transfer rate could be realized without a drastic change of disk structure.

ACKNOWLEDGMENTS

This work were supported by the Ministry of Education of the Republic of China with the Academic Center of Excellence in "Photonics Science and Technology of Tera Era" under Contract No. 89-E-FA06-1-4 as well as the National Science Council of the Republic of China under contract No. NSC92-2216-E-009-013.

[1] R. E. Reed-Hill, *Physical Metallurgy Principles*, 2nd ed. (Van Nostrand, New York, 1991), p. 408.
[2] D. A. Porter and K. E. Easterling, *Phase Transformations in Metals and Alloys*, 2nd ed. (Chapman and Hall, New York, 1992), p. 263.
[3] E. R. Meinders, H. J. Borg, M. H. R. Lankhorst, J. Hellmig, and A. V. Mijiritskii, J. Appl. Phys. **91**, 9794 (2002).
[4] L. H. Chou and Y. Y. Chang, Jpn. J. Appl. Phys., Part 1 **40**, 1272 (2001).
[5] T. Kato, H. Hirata, T. Komaki, H. Inoue, H. Shingai, N. Hayashida, and H. Utsunomiya, Jpn. J. Appl. Phys., Part 1 **41**, 1664 (2002).
[6] G. F. Zhou and B. A. J. Jacobs, Jpn. J. Appl. Phys., Part 1 **38**, 1625 (1999).
[7] B. Tieke, M. Dekker, N. Pfeffer, R. V. Woudenberg, G. F. Zhou, and I. P. D. Ubbens, Jpn. J. Appl. Phys., Part 1 **39**, 762 (2000).
[8] N. Nobukuni, M. Takashima, T. Ohno, and M. Horie, J. Appl. Phys. **78**, 6980 (1995).
[9] H. W. Chen, T. E. Hsieh, J. R. Liu, and H. P. D. Shieh, Jpn. J. Appl. Phys., Part 1 **38**, 1691 (1999).
[10] H. Inoue, H. Hirata, T. Kato, H. Shingai, and H. Utsunomiya, Jpn. J. Appl. Phys., Part 1 **40**, 1641 (2001).
[11] N. Yamada, Proc. SPIE **3109**, 28 (1997).
[12] X. S. Miao, T. C. Chong, L. P. Shi, P. K. Tan, J. M. Li, and K. G. Lim, Jpn. J. Appl. Phys., Part 1 **40**, 1581 (2001).
[13] DVD Forum, *The DVD Specifications for Re-recordable Disc* (Version 1.0, 1999), p. PHX-G2.
[14] T. H. Jeong, M. R. Kim, H. Seo, J. W. Park, and C. Yeon, Jpn. J. Appl. Phys., Part 1 **39**, 2775 (2000).
[15] H. Seo, T. H. Jeong, J. W. Park, C. Yeon, S. J. Kim, and S. Y. Zkim, Jpn. J. Appl. Phys., Part 1 **39**, 754 (2000).
[16] H. E. Kissinger, Anal. Chem. **29**, 1702 (1957).